2024 European Control Conference (ECC)
June 25-28, 2024. Stockholm, Sweden

Rigid Formation Geometry Based Station Keeping by Fixed Speed Vehicles without Self-Location Information

Barış Fidan[1] and Ahmed Fahim Mostafa[1]

***Abstract*— This paper studies a rigid graph theory and distance geometry-based approach to the autonomous vehicle station-keeping problem for situations where global positioning is not available. We propose a control scheme for the station keeping of an autonomous vehicle A, i.e., the task of navigating A to a target point T whose distances are predefined from a set of beacons, where A is not capable of measuring its self-position. The beacons can be stations or other autonomous vehicles, and A is assumed to have nonholonomic unicycle motion kinematics and can measure only distances to the beacons. In the proposed control scheme, the vehicle-beacon range measurements are mapped to the estimate of the distance to T utilizing notions of globally rigid graphs for guaranteeing unique estimation, short-term odometry, and triangulation techniques. The overall scheme involves a target pursuit control law, which can be selected in switching or linear quadratic optimal forms to regulate this distance estimate to zero. Besides formal analysis of the range estimation scheme and discussion of real-time implementations, the performance of the proposed control scheme is verified by simulation tests.**

I. Introduction

Various multi-vehicle or multi-mobile-robot-agent formation control algorithms require an autonomous vehicle (mobile robot) to satisfy certain inter-vehicle geometric constraints with the other vehicles in the network, which usually occur in the form of inter-vehicle distances and/or bearing angles. An example of these objectives for an autonomous vehicle A is *station keeping*, viz. the task of merging it to a multi-vehicle network $S_1, \ldots, S_N$ via converging to a location T that is at a certain distance d_i^* from each (station) vehicle S_i in the existing network. In some cases, the vehicle A is required to converge to T utilizing only its distance measurements to the station vehicles S_i in the control law, in cases where the target location p_T and the location p_i of S_i are not available. Station keeping has applications in other areas, such as sensor network (SN) localization (location estimation), and is studied in a collection of works [1]–[8].

In [1], [2], the station-keeping problem for the case where the self-position p_A of vehicle A is available is approached using adaptive control and optimization techniques. The works [4], [8] treat the station-keeping problem as formation maintenance in multi-agent networks and propose an adaptive solution that first estimates the unknown locations p_i of the stations and then drives the vehicle A toward the target T utilizing a gradient convex minimization algorithm proposed in [9] for range-based SN localization. The works [4], [8] assume that the vehicle A is a holonomic vehicle with known position p_A, similarly to [1], [2].

Two other closely relevant control problems that localizqtion of a target through range measurements and navigating an autonomous vehicle to the vicinity of the unknown target location are *adaptive target pursuit* [10], viz. reaching to the target point, and *adaptive circumnavigation* [11], viz. settling on a circular close orbit around the target point. These problems have been studied in [10]–[13] for the case where the autonomous vehicle has access to its self-location.

The adaptive circumnavigation, adaptive pursuit, and station-keeping problems for the case where the autonomous vehicle cannot measure its location have later been studied in [5], [6], [14]. Inspired by [14], the works [5]–[7] have proposed switching-based solutions to the adaptive target pursuit and station-keeping problems for the case with lack of the autonomous vehicle's self-location information, where a nonholonomic motion kinematics model is used for the vehicle. The adaptive target pursuit controller proposed in [5], [6] uses the range measurement to the target as a feedback signal and tunes the angular velocity of the vehicle so that this signal decays to (a small neighborhood of) zero. The station-keeping control design in the same works uses the same idea and tunes the vehicle's angular velocity in a way to minimize a cost penalizing the difference between actual and desired vehicle-station distances.

Later, to address the agent path and motion optimality, a linear quadratic (LQ) optimal target pursuit and station-keeping control schemes involving a Luenberger observer-based state estimator are designed in [7]. Although the station keeping control approaches in [5]–[7] are justified to work in general, the proposed algorithms are influenced by the indirect approach aiming to minimize multiple vehicle-station distance errors simultaneously, and as a consequence, the produced navigation paths are not optimal.

Aiming to address these issues, we propose a new approach integrating the switching adaptive target pursuit controller of [5], [6] or the LQ optimal pursuit controller of [7] with a rigid formation geometry-based estimator to generate an estimate $\hat{r}$ of the vehicle distance $r = \|p_A - p_T\|$ to the target location T which is at pre-specified distances d_i^* from the station vehicles or nodes S_i and short-term integral odometry to estimate the displacement d_A of A between two sample instants. d_A is required for the triangulation procedure of the proposed vehicle-target distance estimator, and the uniqueness and accuracy of the generated estimate for ideal noise-free distance measurement cases are guaranteed by utilizing notions of globally rigid graphs.

[1]B. Fidan and A. F. Mostafa are with the Department of Mechanical and Mechatronics Engineering, University of Waterloo, Canada. fidan@uwaterloo.edu, ahmedfahim@ieee.org
This work is supported by the Canadian NSERC Discovery Grant 116806.

The paper is organized as follows. In Section II, we define the station-keeping problem. In Section III, we propose the overall control scheme and propose our vehicle-target range estimation method. In Section IV, we present a set of simulation test results. The implementation aspects of the proposed control scheme are discussed in Section V. Concluding remarks are provided in Section VI.

II. Station Keeping Problem

Consider an autonomous vehicle A with nonholonomic agent kinematics

$$\dot{x}_A = v\cos(\theta), \quad \dot{y}_A = v\sin(\theta), \quad \dot{\theta} = \omega, \tag{1}$$

where $p_A(t) \triangleq [x_A(t),\ y_A(t)]^\top \in \Re^2$ is the position of A in a global frame, $\theta(t) \in (-\pi, \pi]$ is the global heading angle, and $u(t) \triangleq [v(t),\ \omega(t)]^\top \in \Re^2$ is the control input of the vehicle. The control signals v, ω represent the linear and angular speeds of the vehicle, respectively, satisfying $0 \le v \le \bar{v}$ and $|\omega| \le \bar{\omega}$ for some $\bar{v}, \bar{\omega} > 0$.

Consider also an SN $\mathcal{S} = \{S_1, \cdots, S_N\},\ N \ge 3$, which represents either (i) a vehicle network A is required to merge in, where each S_i denotes a vehicle or (ii) a sensory station network. Let T be an unknown target point having distance d_i^* from each S_i, which denotes the desired distance of A to each vehicle in scenario (i), or the distance of a signal source (located at T) measured by sensory station S_i in scenario (ii). The station-keeping task of A is to reach T using the available range measurements. Using $\mathcal{B}_{\epsilon_r}(p_T)$ to denote the ϵ_r neighborhood of the position p_T, i.e., the disc with center p_T and radius ϵ_r, this task can be formally defined as follows:

Problem 1: Consider a nonholonomic vehicle A with motion kinematics (1) and a set of N sensor stations $\mathcal{S} = \{S_1, \cdots, S_N\},\ N \ge 3$ located at unknown positions $p_1, \ldots, p_N \in \Re^2$. Let T be a target point located at an unknown constant position $p_T = [x_T,\ y_T]^\top \in \Re^2$ and has known distances $\|p_i - p_T\| = d_i^*,\ i = 1, \ldots, N$, from the stations. Assume that p_i are not collinear, and A is informed with the target distances d_i^* and the actual vehicle-station distances $\|p_i - p_A(t)\| = d_i(t)$ for all $t \ge 0$. Design a control law $u = [v(t),\ \omega(t)]^\top$ that drives A to an ϵ_r neighborhood $\mathcal{B}_{\epsilon_r}(p_T)$ of T in finite time for some $\epsilon_r > 0$.

The dynamics (1) is not suitable for the objectives presented in the sequel because the vehicle A cannot measure any of the state variables $x_A,\ y_A,\ \theta$, nor p_T. Similar to [5]–[7], instead of (1), we use the following kinematics model focusing on the range $r(t) \triangleq \|p_A(t) - p_T\|$ and the heading angle $\theta_T \in (-\pi, \pi]$ measured from the $p_A - p_T$ line segment to A's heading, as represented in Fig. 1:

$$\dot{r}(t) = -v(t)\cos(\theta_T(t)), \tag{2}$$

$$\dot{\theta}_T(t) = \omega(t) + \frac{1}{r(t)} v(t)\sin(\theta_T(t)). \tag{3}$$

The distances d_i represent an implicit measure of the range r. In the sequel, we propose a vehicle-target range estimation scheme deploying the geometric properties of a pseudo-SN with nodes located at $p_T, p_1, \ldots, p_N$ and $p_A(t)$ at two consequent sample instants of time t.

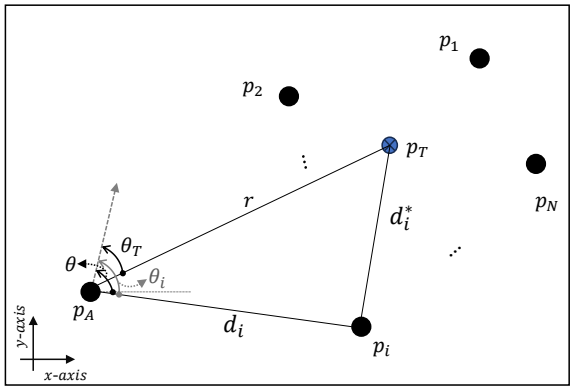

Fig. 1. An example configuration with the vehicle A, the target T and the N sensor stations S_i.

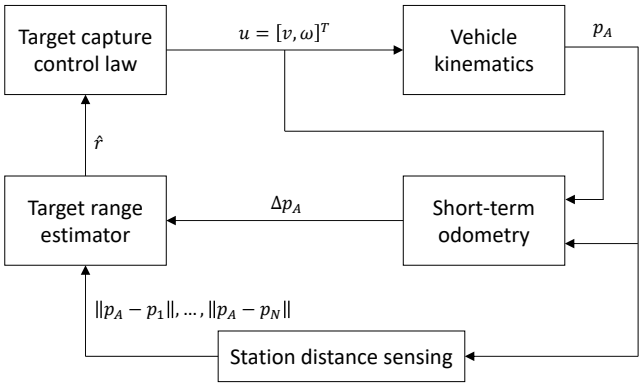

Fig. 2. The block diagram of the overall control scheme.

III. Proposed Control Scheme

The proposed control scheme for solving Problem 1 is composed of three main components; a short-term integral odometry scheme for calculation of the displacement $d_{Ak} = \|\Delta p_A[k]\| = \|p_A[k] - p_A[k-1]\|$ between the vehicle locations $p_A[k-1] = p_A((k-1)T_0)$ and $p_A[k] = p_A(kT_0)$ and at consequent sampling times, assuming a fixed sampling time $T_0 > 0$ that is long enough for acceptable odometry accuracy, a rigid formation geometry based vehicle-target range estimator, and a target capture control law proposed in [5], [6], as depicted in Fig. 2. The "Target capture control law" can be chosen as an adapted version of either the switching-based control scheme of [5], [6], or the LQ optimal control scheme of [7] and aims to regulate the estimate $\hat{r}$ of the vehicle-target range r to (a small value close enough to) zero. The accuracy of the estimate $\hat{r}$ is crucial for the performance of the overall station-keeping scheme.

In Fig. 2, the "Vehicle kinematics" block represents the non-holonomic kinematics (1) of the vehicle. The "Target range estimator" utilizes the distance geometry among the sensor stations $S_1, \ldots, S_N$, the target T, and two instant locations of the vehicle A (at two consequent sampling times) to generate the estimate $\hat{r}$ based on the rigidity of the formed graph, as detailed in the next subsection.

A. Rigid Graph Theory Based Target Range Estimation

In this subsection, we propose an algorithm to estimate the unknown distance $r(t)$ between the agent location $p_A(t)$ and the target location p_T at each sampling time $t = kT_0$ for $k = 1, 2, \ldots$, given the station-target distances $\|p_i - p_T\| = d_i^*$, the range measurements of $\|p_A(t) - p_i\| = d_i(t)$ at the time instants $t = kT_0$ and $t = (k-1)T_0$ (denoted by d_{ik} and $d_{i(k-1)}$, respectively), and the short-term odometry based measurement of the displacement d_{Ak} of A from $p_A[k-1] = p_A((k-1)T_0)$ to $p_A[k] = p_A(kT_0)$. Leaving discussions on the measurement noise effects to Section V, let us assume that range and displacement measurements are accurate.

The setting of the above estimation problem fits well with distance graph theory-based SN localization, where a planar SN is represented by a graph $\mathcal{G}_{SN} = (\mathcal{V}_{SN}, \mathcal{E}_{SN})$, called the *underlying graph* of the SN, each vertex in $\mathcal{V}_{SN}$ representing a sensor node and each edge in $\mathcal{E}_{SN}$ representing a node pair with known inter-distance. For estimation of r, at each sampling time $t = kT_0$ for $k = 1, 2, \ldots$, we consider a pseudo-SN with $N + 3$ nodes ($N \geq 3$) located at $p_1, \ldots, p_N, p_T, p_A[k], p_A[k-1]$, which are all unknown, as illustrated in Figure 3, and represented, respectively, by vertices $\mathsf{v}_1, \ldots \mathsf{v}_N, \mathsf{v}_T, \mathsf{v}_{A0}, \mathsf{v}_{A1}$. Considering the available inter-node distance measurements to determine the edges, the underlying graph of this pseudo-SN is defined as

$$\begin{aligned} \mathcal{G} =& (\mathcal{V}, \mathcal{E}),\ \mathcal{V} = \{\mathsf{v}_1, \ldots \mathsf{v}_N, \mathsf{v}_T, \mathsf{v}_{A0}, \mathsf{v}_{A1}\}, \qquad (4) \\ \mathcal{E} =& \{(\mathsf{v}_1, \mathsf{v}_T), \ldots, (\mathsf{v}_N, \mathsf{v}_T), (\mathsf{v}_1, \mathsf{v}_{A0}), \ldots, (\mathsf{v}_N, \mathsf{v}_{A0}), \\ & (\mathsf{v}_1, \mathsf{v}_{A1}), \ldots, (\mathsf{v}_N, \mathsf{v}_{A1}), (\mathsf{v}_{A0}, \mathsf{v}_{A1})\}. \end{aligned}$$

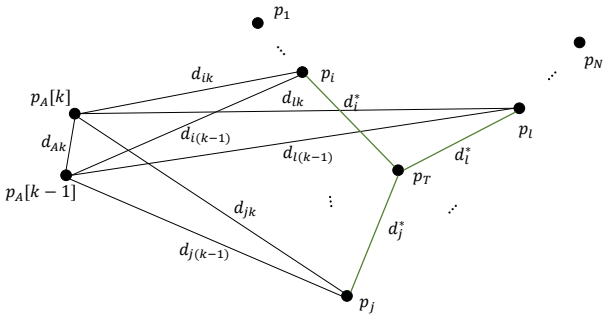

Fig. 3. The pseudo-sensor network and its underlying graph for the target range estimation problem: $1 \leq i < j < l \leq N$.

Next we establish that each of the target distances $r_k = \|p_A[k] - p_T\|$ and $r_{k-1} = \|p_A[k-1] - p_T\|$ is uniquely determined given the distances corresponding to the edges in $\mathcal{E}$, utilizing the notion of *global rigidity* [15], [16]. To formally define *global rigidity* [19], we need to introduce some rigid graph and matroid theory notions first: A 2D *framework* (G, π) is a pair of a graph $G = (V, E)$ and a map π, called *realization*, from V to $\Re^2$. A 2D realization is called *generic* if the mappings for any three vertices in V are non-collinear. Two 2D frameworks (G, π) and (G, ϱ) are called *equivalent* if $\|\pi(\mathsf{u}) - \pi(\mathsf{v})\| = \|\varrho(\mathsf{u}) - \varrho(\mathsf{v})\|$ for any $(\mathsf{u}, \mathsf{v}) \in E$, and are called *congruent* if $\|\pi(\mathsf{u}) - \pi(\mathsf{v})\| = \|\varrho(\mathsf{u}) - \varrho(\mathsf{v})\|$ for any $\mathsf{u}, \mathsf{v} \in V$. (G, π) is called *rigid* if there exists $\varepsilon > 0$ such that any (G, ϱ) that is equivalent to (G, π) and satisfies $\|\pi(\mathsf{v}) - \varrho(\mathsf{v})\| < \varepsilon,\ \forall \mathsf{v} \in V$ is congruent to (G, π). (G, π) is called *globally rigid* if every framework equivalent to (G, π) is congruent to (G, π). Rigidity and global rigidity are generic graph properties, i.e. given any two generic realizations π and ϱ of a graph G, (G, π) is (globally) rigid if and only if (G, ϱ) is (globally) rigid. A graph G is called *generically (globally) rigid* in 2D if any 2D framework (G, π) is (globally) rigid. A generically rigid graph $G = (V, E)$ is called *generically redundantly rigid* if G remains rigid after removal of any single edge from E.

Consider the 2D framework $(\mathcal{G}, p)$, where $\mathcal{G}$ is as defined in (4) and p maps $\mathsf{v}_1, \ldots \mathsf{v}_N, \mathsf{v}_T, \mathsf{v}_{A0}, \mathsf{v}_{A1}$ to $p_1, \ldots p_N$, $p_T, p_A[k], p_A[k-1]$, respectively. All the inter-node distances for this framework, including r_k and r_{k-1}, are uniquely determined if $\mathcal{G}$ is generically globally rigid in 2D. The next proposition establishes 2D generic global rigidity of $\mathcal{G}$.

Proposition 1: For $N \geq 3$, the graph $\mathcal{G} = (\mathcal{V}, \mathcal{E})$ defined in (4) is generically globally rigid in 2D.

Proof: A graph is generically globally rigid in 2D if it is generically redundantly rigid and vertex-3-connected [20]. $\mathcal{G}$ defined in (4) is both generically redundantly rigid and vertex-3-connected. ■

Utilizing Proposition 1 for guaranteeing solution existence and uniqueness, one can design different sequential combinatorial algorithms or batch optimization algorithms to calculate all the edge distances for $\mathcal{G}$ [15], [17], [18]. One example sequential algorithm is provided in Algorithm 1 to generate the estimate $\hat{r}_k$ and $\hat{r}_{k-1}$ of r_k and r_{k-1}, respectively. In Algorithm 1, a local coordinate frame is considered with $p_A[k-1] = p_{A1}$ at the origin $(0, 0)$ and $p_A[k] = p_{A0}$ at $(0, d_{Ak})$. Three of the available distance measurements are chosen, denoted d_i, d_j, d_l, based on certain robustness criteria (see Remark 1). Next, two possible beacon positions are calculated for each of p_i, p_j, p_l applying a standard triangulation routine (lines 2-4). Then, without loss of generality, two of the three desired distance values d_i^*, d_j^* are chosen from which (at most) four possible target locations are calculated (lines 6-9). Finally, the possible target locations are evaluated based on fit with d_l^* and the two possible locations for p_l in lines 11–14, and the vehicle-target distance at time instants $t = kT_0$ and $t = (k+1)T_0$ are estimated in lines 15–18.

Remark 1: Although three beacons suffice to guarantee the uniqueness of $\hat{r}_k$ and $\hat{r}_{k-1}$, we consider the general case $N \geq 3$ to increase the flexibility and robustness of our algorithm. At any time instant, the mobile vehicle utilizes distance measurements to only three beacons which can be chosen based on the quality of the measurement signal. For instance, if $N > 3$ and the deviation of measurements to a particular beacon is too high, the vehicle can discard that beacon's measurement to improve robustness.

Algorithm 1 Estimation of $\hat{r}$

Require: $d_{Ak}, d_{1k}, \ldots, d_{Nk}, d_{1(k-1)}, \ldots, d_{N(k-1)}$, $d_1^*, \ldots, d_N^*$

Ensure: $\hat{r}_k, \hat{r}_{k-1}$

$(p_{A1}, p_{A0}) \leftarrow ((0,0),(0,d_{Ak}))$
$\{p_i^1, p_i^2\} \leftarrow$ TRIANGULATE$(p_{A1}, p_{A0}, d_{i(k-1)}, d_{ik})$
$\{p_j^1, p_j^2\} \leftarrow$ TRIANGULATE$(p_{A1}, p_{A0}, d_{j(k-1)}, d_{jk})$
$\{p_l^1, p_l^2\} \leftarrow$ TRIANGULATE$(p_{A1}, p_{A0}, d_{l(k-1)}, d_{lk})$
$\mathrm{P_T} \leftarrow \emptyset$
for $q_i = 1:2$ **do**
  for $q_j = 1:2$ **do**
    $\{p_{T1}, p_{T2}\} \leftarrow$ TRIANGULATE$(p_i^{q_i}, p_j^{q_j}, d_i^*, d_j^*)$
    Append $\mathrm{P_T}$ with p_{T1}, p_{T2}
$\hat{r}_k \leftarrow \infty, \quad \hat{r}_{k-1} \leftarrow \infty$
$q_{l1} = \arg\min_{q=1:\ \mathrm{length}(\mathrm{P_T})} |\|p_l^1 - \mathrm{P_T}[q]\| - d_l^*|$
$L_1 = |\|p_l^1 - \mathrm{P_T}[q_{l1}]\| - d_l^*|$
$q_{l2} = \arg\min_{q=1:\ \mathrm{length}(\mathrm{P_T})} |\|p_l^2 - \mathrm{P_T}[q]\| - d_l^*|$
$L_2 = |\|p_l^2 - \mathrm{P_T}[q_{l2}]\| - d_l^*|$
if $L_1 < L_2$ **then**
  $\hat{r}_k \leftarrow \|\mathrm{P_T}[q_{l1}] - p_{A_0}\|, \quad \hat{r}_{k-1} \leftarrow \|\mathrm{P_T}[q_{l1}] - p_{A_1}\|$
else
  $\hat{r}_k \leftarrow \|\mathrm{P_T}[q_{l2}] - p_{A_0}\|, \quad \hat{r}_{k-1} \leftarrow \|\mathrm{P_T}[q_{l2}] - p_{A_1}\|$

B. Odometry Based Displacement Calculation

Here, we propose an odometry-based periodic calculation of vehicle motion that is robust and easily implementable on real-time systems. We denote by T_o the *fixed odometry period* and denote by $\theta^{'}$ the *reset heading angle* such that $\theta^{'}(t_0) = 0$ and $\theta^{'}(t) = \theta(t) - \theta(t_0)$ for $t_0 \le t < kT_0$, for any $t_0 = (k-1)T_0$ and $k = 1, 2, \ldots$ The vehicle A does not have direct access to $\theta^{'}$ because the heading $\theta(t)$ is not available to A. We calculate $\theta^{'}$ within $t_0 = (k-1)T_0 \le t < kT_0$ by integrating the angular velocity, i.e.,

$$\theta^{'}(t) = \int_{t=t_0}^{t} \omega(\tau)\mathrm{d}\tau, \tag{5}$$

which can be approximated in discrete time steps with small approximation errors in real implementations.

The vectoral displacement $\Delta p_A[k] := p_A[k] - p_A[k-1]$ of A from $t_0 = (k-1)T_0$ to kT_0 is calculated as $\Delta p_A^m[k]$via odometry considering a local coordinate frame with origin at $p_A[k-1] = p_A(t_0)$ and $+x$-axis in the direction of $\theta(t_0)$ as follows:

$$\Delta p_A^m[k] = \int_{t=t_0}^{kT_o} \dot{p}_A(t)\mathrm{d}t = \bar{v} \begin{bmatrix} \int_{t=t_0}^{kT_o} \cos(\theta^{'}(t))\mathrm{d}t \\ \int_{t=t_0}^{kT_o} \sin(\theta^{'}(t))\mathrm{d}t \end{bmatrix}. \tag{6}$$

C. Target Capture Control Law

As mentioned earlier, the "target capture control law" in Fig. 2 aims to regulate the estimate $\hat{r}_k$ of the vehicle-target range r, which is generated by the range estimator described in Section III-A, to zero, and can be chosen as an adapted version of either the switching based control scheme of [5], [6] or the LQ optimal control scheme of [7]. Here we briefly describe each of these two options.

As the first option, application of the switching target capture control law based on [5], [6] utilizes a fixed approximation $\rho_k := (\hat{r}_k - \hat{r}_{k-1})/T_0$ of $\dot{\hat{r}}(t)$ within each time interval $[kT_0, (k+1)T_0)$, leading to the following triangulation range estimation based switching (T-switching) control scheme for $kT_0 \le t < (k+1)T_0$:

$$u = [v,\ \omega]^\top, \tag{7}$$

$$v(t) = \begin{cases} \bar{v}, & \text{if } \hat{r}_k > \epsilon_r \\ 0, & \text{otherwise,} \end{cases} \tag{8}$$

$$\omega(t) = \begin{cases} \left(\mathrm{sgn}(\rho_k) + 1 + \dfrac{(1+\alpha)\bar{v}}{\hat{r}_k}\right)\sigma\left(\dfrac{-\rho_k}{\bar{v}}\right), & \text{if } \hat{r}_k > \epsilon_r \\ 0, & \text{otherwise,} \end{cases} \tag{9}$$

where α is a design parameter satisfying

$$0 < \alpha < \frac{\epsilon_r(\bar{\omega} - 2)}{\bar{v}} - 1, \tag{10}$$

and σ is a function that defines the characteristics of the transitions of ω at different θ_T profiles and is used to penalize the deviation of θ_T from its desired value zero. An example σ function is given in [5], [6] as follows:

$$\sigma(x) = \begin{cases} 1, & \text{if } x \le \sqrt{1-\gamma} \\ \frac{1-x^2}{\gamma}, & \text{if } \sqrt{1-\gamma} < x < 1 \\ 0, & \text{if } x \ge 1 \end{cases} \tag{11}$$

where $0 < \gamma < 1$. Note that the control law (9)–(11) guarantees that $0 \le \omega \le \bar{\omega}$. Under the control law (7)-(9), the vehicle agent A moves with constant linear speed $\bar{v} > 0$ and non-negative angular speed ω till $\hat{r}_k$ gets smaller than ϵ_r. Particularly, (9) guides A to rotate with a rate dependent on $\hat{r}_k$, $\bar{v}$, and the sign of ρ_k as long as A is estimated to be outside the target vicinity ball $\mathcal{B}_{\epsilon_r}(p_T)$, unless $|\theta_T|$ gets sufficiently close to zero. The switches to zero in the control inputs (8) and (9) prevent chattering and assure that the vehicle stops once A is estimated to enter the disc $\mathcal{B}_{\epsilon_r}(p_T)$.

As the second option, the triangulation estimation-based LQ (T-LQ) optimal control scheme based on [7] keeps the lines (7) and (8) in the above control scheme but replaces (9) with the following state-space LQ optimal control law that aims to minimize the quadratic cost function

$$J = \frac{1}{2}\int_0^\infty [x^T(t)Q_c x(t) + r_c\omega^2(t)]\ dt, \tag{12}$$

with positive definite state cost matrix Q_c and positive input cost scalar r_c, for the equivalent state space representation

$$\dot{x}(t) = \underbrace{\begin{bmatrix} -\bar{v}\cos x_2(t) \\ \frac{\bar{v}\sin x_2(t)}{x_1(t)} \end{bmatrix}}_{f(x(t))} + \underbrace{\begin{bmatrix} 0 \\ 1 \end{bmatrix}}_{B}\omega(t) \tag{13}$$

of (2),(3) with state $x(t) = [r(t),\ \theta_T(t)]^T$, for the cases where $v(t) = \bar{v}$, i.e., $\hat{r}_k > \epsilon_r$, fed by an estimate $\hat{x}$ of the state, noting unavailability of the measurement of θ_T:

$$\omega(t) = -K_c(t)\hat{x}(t), \tag{14}$$

$$K_c(t) = r_c^{-1}B^T P(t), \tag{15}$$

where $P_c = P_c^T > 0$ is the solution of the Riccati equation

$$\begin{aligned} \dot{P}_c &= P_c A_c^T + A_c P_c - P_c B r_c^{-1} B^T P_c + Q_c = 0, \\ A_c &= \left.\frac{\partial f}{\partial x}\right|_{\hat{x}} = \begin{bmatrix} 0 & \bar{v}\sin\hat{x}_2 \\ \frac{-\bar{v}\sin\hat{x}_2}{\hat{x}_1^2} & \frac{\bar{v}\cos\hat{x}_2}{\hat{x}_1} \end{bmatrix}, \ \hat{x}_1 \neq 0, \end{aligned}$$

with derivation details provided in [7], and $\hat{x}$ is obtained as mapping of the estimate $\hat{x}_o$ of the 3-dimensional state $x_o = [r^2/2, \ r\sin\theta_T, \ r\cos\theta_T]^T$ of the model

$$\begin{aligned} \dot{x}_o &= \underbrace{\begin{bmatrix} 0 & 0 & -\bar{v} \\ 0 & 0 & \omega \\ 0 & -\omega & 0 \end{bmatrix}}_{\bar{A}(\omega)} x_o + \underbrace{\begin{bmatrix} 0 \\ 0 \\ -\bar{v} \end{bmatrix}}_{\delta} = f(x_o, \ \omega), \\ y_o &= x_{o1} = \underbrace{\begin{bmatrix} 1 & 0 & 0 \end{bmatrix}}_{C^T} x_o, \end{aligned}$$

which is equivalent to (13), by the Luenberger observer

$$\dot{\hat{x}}_o = \bar{A}(\omega)\hat{x}_o + \delta + K_o(\omega)(y_o - C^T\hat{x}_o),$$

where the observer gain $K_o(\omega)$ is calculated so that the dynamics of the state estimation error $\hat{x}_o - x_o$ has the desired stable eigenvalues, and the required output $y_o(t)$, within each time interval $kT_0 \leq t < (k+1)T_0$, is approximated as

$$y_o(t) \approx r_k^2/2.$$

IV. Simulations

The proposed station-keeping scheme, summarized in Figure 2, with both the switching implementation (7),(8),(9) and the LQ optimal implementation (7),(8),(14) of the "target capture control law", is numerically tested through various simulations. The results for a case with three station sensors $S_1, \ S_2, \ S_3$ located at $p_1 = [-0.4, \ -0.2]^T$, $p_2 = [0.4, \ 0]^T$, $p_3 = [0, \ 0.5]^T$, and T located at $p_T = [0, \ 0]^T$ are shown in Figures 4–7. The vehicle agent A starts motion from $p_A(0) = [-4, \ -1.5]^T$ with an initial orientation angle $\theta(0) = \pi/3$. Using a fixed-time step to allow the calculation of the odometry-based displacement (6), the subsequent positions of the mobile agent are used to facilitate the execution of the proposed target range algorithmic steps detailed in the pseudo-code of Algorithm 1.

The trajectories of the mobile agent under the proposed triangulation estimation-based switching (T-switching) and LQ (T-LQ) optimal control schemes, which incorporate the target range estimator of Section III-A, are shown in Fig. 4. The same figure displays the trajectory obtained via the original LQ optimal station keeping control scheme of [7] as well, for comparison purposes. The performance enhancement via the T-LQ optimal approach can be easily observed in terms of the length of the agent trajectory and the smoothness and amplitude of the control signal ω. The control inputs shown in Fig. 5, Fig. 6 and Fig. 7 provide the change of the angular velocity input with respect to time, which can be corresponded to the smoothness of the vehicle trajectory and the practicality of the control scheme. Fig. 7 shows the aggressive fluctuation of the angular velocity due to the dependence on the different errors calculated with respect to each beacon. Such fluctuation causes the irregularity of the final generated path, as in both cases of using the original switching station keeping control scheme of [6] or the original LQ optimal station keeping control scheme of [7]. These adverse effects are well eliminated utilizing the target range estimator of Section III-A.

V. Discussion on Real Time Implementations

The proposed station-keeping scheme of Figure 2, with both switching and LQ optimal implementations of the "target capture control law", is practical and easily implementable in real-time applications. The proposed scheme requires the utilization of the onboard sensing capabilities of a mobile robot solely and does not depend on a fixed infrastructure or a ground station. Particularly, the vehicle (or mobile robot) A only needs an onboard sensor that provides distance measurements to the stations $S_1, \ldots, S_N$ and a simple odometry unit. Several types of sensors can be used to obtain A-S_i distance measurements. For instance, if the stations S_i are equipped with ultrawideband (UWB) range sensors or wireless radio transmitters, then a receiver of the same kind of sensor can be utilized on board of A. Various distance estimation schemes are available for such settings, including received signal strength (RSS), time-of-arrival (TOA), and time-difference-of-arrival (TDOA) based ones. If the stations S_i are passive, i.e., they do not actively transmit signal, then a light detection and ranging (LIDAR) sensor or a low-cost combination of a laser range sensor and a monocular camera can be used to measure the distance with additional feature detection/identification algorithms. Odometry data is easily obtained by wheel encoders in nonholonomic ground robots or by inertial measurement unit (IMU) sensors in fixed-wing UAVs up to a certain error level. Since typical research/commercial robots are already equipped with most of these sensors in common robotics applications, our algorithm can be readily applied to these robots to aid in navigation in GPS-denied environments.

VI. Conclusion

We have proposed a new station-keeping control scheme. for nonholonomic autonomous vehicles without access to

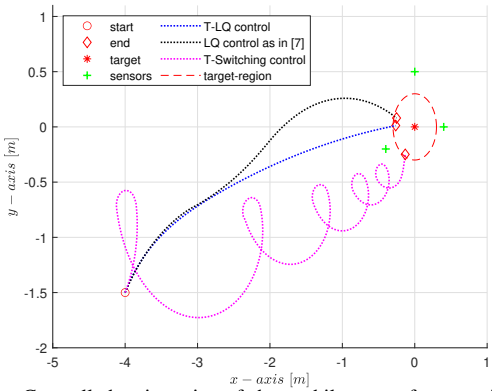

Fig. 4. Controlled trajectories of the mobile agent for a station-keeping simulation with target range estimation.

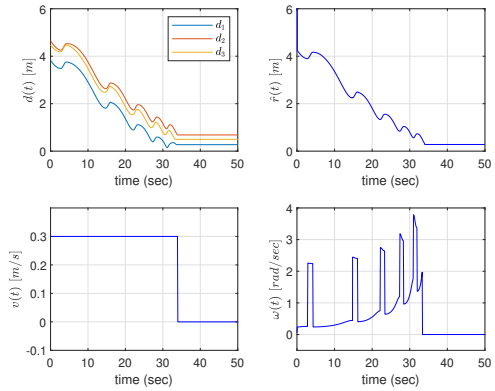

Fig. 5. $d(t)$, $\hat{r}(t)$, $v(t)$, $\omega(t)$ for the simulated station keeping problem with the switching controller and target range estimation.

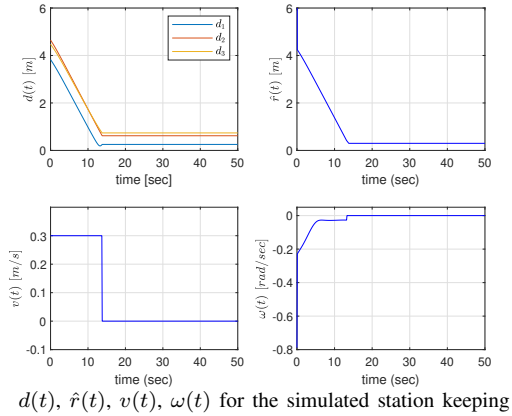

Fig. 6. $d(t)$, $\hat{r}(t)$, $v(t)$, $\omega(t)$ for the simulated station keeping problem with the LQ optimal controller and target range estimation.

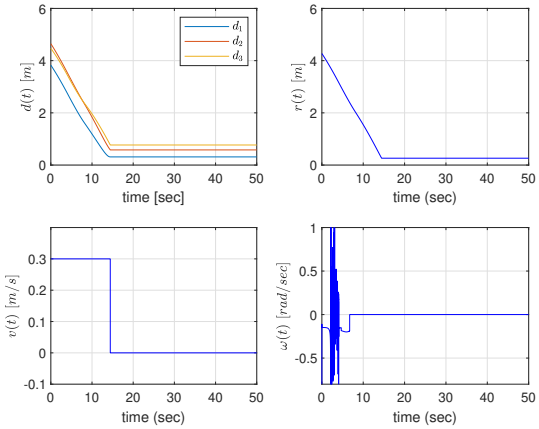

Fig. 7. $d(t)$, $r(t)$, $v(t)$, $\omega(t)$ for the simulated station keeping problem with the LQ optimal controller.

global position information, mapping the station-keeping problem to a target capture problem using a rigid formation theory and distance geometry-based target range estimation algorithm. The proposed scheme first generates the range estimate that is implicitly defined in the rigid graph constructed at certain time intervals by the stations, the target, and two instances of the vehicle position. Then, this estimate is fed to the control law for the mapped target capture problem to drive the vehicle toward the target by using only this estimate. Implementations of the target capture control law via switching and LQ optimal approaches are studied. In the considered setting, the target location, station locations, and the vehicle's self-location are not available. Therefore, the proposed scheme constitutes a promising approach for the cases the vehicle cannot locate the stations or the target but can measure distances to the stations. A planned follow-up future work is to analyze and enhance robustness of the overall control scheme to sensor noises and to implement it in real-time with ground and aerial autonomous vehicles.

REFERENCES

[1] M. Cao and A.S. Morse , "Station keeping in the plane with range-only measurements, " *American Control Conf.,* pp.5419-5424, July 2007.

[2] M. Cao and A. S. Morse, "An adaptive approach to the range-only station-keeping problem, " *Int. J. Adapt. Control Signal Process,* vol.26, pp. 757–777, February 2012.

[3] B. Fidan, S. Dasgupta, and B.D.O. Anderson, "Realistic anchor positioning for sensor localization, " in *Recent advances in learning and control,* V.D. Blondel, S.P. Boyd, and H. Kimura (ed.), Springer-Verlag, pp. 79–94, 2008.

[4] S. Güler, B. Fidan, S. Dasgupta, B.D.O. Anderson, and I. Shames, "Adaptive source localization based station keeping of autonomous vehicles, " *IEEE Tr. Automatic Control,* vol. 62, no. 7, pp. 3122–3135, July 2017.

[5] S. Güler and B. Fidan, "Range based target capture and station keeping of nonholonomic vehicles without GPS, " *Proc. European Control Conference,* pp. 2970–2975, July 2015.

[6] S. Güler and B. Fidan, "Target capture and station keeping of fixed speed vehicles without self-location information, " *European Journal of Control,* vol. 43, pp. 1-11, 2018.

[7] A. F. Mostafa and S. Güler and B. Fidan, "Optimal target capture and station keeping control of mobile agents without global position information, " *Proc. European Control Conference,* pp. 1–6, July 2023.

[8] S. Güler, *Adaptive Formation Control of Cooperative Multi-Vehicle Systems,* PhD Thesis, University of Waterloo, 2015.

[9] B. Fidan and F. Kiraz, "On convexification of range measurement based sensor and source localization problems, " *Ad Hoc Networks,* vol.20, pp. 113–118, April 2014.

[10] B. Fidan, S. Dasgupta, and B.D.O. Anderson, "Adaptive range-measurement-based target pursuit, " *Int. J. Adapt. Control Signal Process,* vol.27, pp. 66–81, 2013.

[11] I. Shames, S. Dasgupta, B. Fidan, and B.D.O. Anderson, "Circumnavigation using distance measurements under slow drift, " *IEEE Trans. Automatic Control,* vol.57, no.4, pp. 889–903, April 2012.

[12] J. Cochran and M. Krstic, "Nonholonomic source seeking with tuning of angular velocity, " *IEEE Trans. on Automatic Control,* vol.54, no.4, pp. 717–731, April 2009.

[13] A. Matveev, A. Semakova, A. Savkin, "Tight circumnavigation of multiple moving targets based on a new method of tracking environmental boundaries, " *Automatica,* vol. 79, pp. 52–60, March 2017.

[14] Y. Cao, "UAV circumnavigating an unknown target under a GPS-denied environment with range-only measurements, " *Automatica,* vol.55, pp. 150–158, May 2015.

[15] G. Mao and B. Fidan (editors), *Localization Algorithms and Strategies for Wireless Sensor Networks*, IGI Global, 2009.

[16] B. Jackson and T. Jordan, "Graph theoretic techniques in the analysis of uniquely localizable sensor networks," Chapter 6 in *Localization Algorithms and Strategies for Wireless Sensor Networks*, G. Mao and B. Fidan (editors), IGI Global, 2009.

[17] I. Shames, B. Fidan, and B.D.O. Anderson, "Minimization of the effect of noisy measurements on localization of multi-agent autonomous formations," *Automatica,* vol.45, pp. 1058–1065, 2009.

[18] B.D.O. Anderson, I. Shames, G. Mao, and B. Fidan, "Formal theory of noisy sensor network localization," *SIAM Journal on Discrete Mathematics,* vol. 24, no. 2, pp. 684–698, 2010.

[19] R. Connelly, "Generic global rigidity," *Discrete Computational Geometry*, vol. 33, pp. 549–563, 2005.

[20] B. Jackson and T. Jordan, "Connected rigidity matroids and unique realizations of graphs," *J. Combinatorial Theory, Ser. B*, vol. 94, pp. 1–29, 2005.